

Using control to shape stochastic escape and switching dynamics

Cite as: Chaos **29**, 053128 (2019); <https://doi.org/10.1063/1.5090113>

Submitted: 24 January 2019 . Accepted: 09 May 2019 . Published Online: 31 May 2019

Dhanushka Kularatne , Eric Forgoston, and M. Ani Hsieh 



View Online



Export Citation



CrossMark

ARTICLES YOU MAY BE INTERESTED IN

Chaos in a ring circuit

Chaos: An Interdisciplinary Journal of Nonlinear Science **29**, 043103 (2019); <https://doi.org/10.1063/1.5079941>

Practical rare event sampling for extreme mesoscale weather

Chaos: An Interdisciplinary Journal of Nonlinear Science **29**, 053109 (2019); <https://doi.org/10.1063/1.5081461>

Stretches across for chaos

Chaos: An Interdisciplinary Journal of Nonlinear Science **29**, 053127 (2019); <https://doi.org/10.1063/1.5091451>

AIP Author Services
English Language Editing



Using control to shape stochastic escape and switching dynamics

Cite as: Chaos 29, 053128 (2019); doi: 10.1063/1.5090113

Submitted: 24 January 2019 · Accepted: 9 May 2019 ·

Published Online: 31 May 2019



View Online



Export Citation



CrossMark

Dhanushka Kularatne,^{1,a)}  Eric Forgoston,² and M. Ani Hsieh¹ 

AFFILIATIONS

¹Mechanical Engineering and Applied Mechanics, University of Pennsylvania, Philadelphia, Pennsylvania 19104, USA

²Department of Mathematical Sciences, Montclair State University, Montclair, New Jersey 07043, USA

^{a)}Electronic mail: dkul@seas.upenn.edu

ABSTRACT

We present a strategy to control the mean stochastic switching times of general dynamical systems with multiple equilibrium states subject to Gaussian white noise. The control can either enhance or abate the probability of escape from the deterministic region of attraction of a stable equilibrium in the presence of external noise. We synthesize a feedback control strategy that actively changes the system's mean stochastic switching behavior based on the system's distance to the boundary of the attracting region. With the proposed controller, we are able to achieve a desired mean switching time, even when the strength of noise in the system is not known. The control method is analytically validated using a one-dimensional system, and its effectiveness is numerically demonstrated for a set of dynamical systems of practical importance.

Published under license by AIP Publishing. <https://doi.org/10.1063/1.5090113>

Noise is an inherent phenomenon in all physical dynamical systems. Thus, the behavior of a dynamical system under the influence of noise has been a widely studied topic. In particular, the effect of small noise on the stability of a system has generated significant attention in the literature. It has been shown that under the influence of noise, a system can be made to transition out of its deterministically stable states. While these are rare occurrences for small noise, they have a significant impact on the overall behavior of the system. The expected time for such a transition to occur, i.e., the mean switching time, is an important characteristic in such systems. In this work, we show how an external control could be used to enhance or abate this switching behavior and synthesize a feedback control strategy that actively changes the mean switching time to a desired value. This enables one to control the dwell time of the system in a given basin of attraction to a desired value. We analyze the controller using a representative one-dimensional system and demonstrate the controller on a set of dynamical systems with practical importance.

I. INTRODUCTION

The trajectories of a deterministic dynamical system are completely defined by the initial conditions. With initial conditions in the region of attraction of a stable equilibrium, the system is expected to approach the equilibrium state and remain there indefinitely. One

would expect this deterministic behavior to be only slightly altered in the presence of small noise, since switching between stable states would require the system to overcome a large activation barrier. However, one often sees these types of rare noise-induced switching events in a variety of physical and biological systems. A few examples of phenomena that exhibit rare transition events include extinction of disease^{1,2} or species,³ switching between gene states⁴ or magnetization states,⁵ and transitions in ocean flows.^{6,7}

In the presence of noise, the system trajectories are no longer prescribed by the initial conditions. Instead, the behavior of the system is now described by the probability density which indicates the likelihood of achieving a particular system state. With this viewpoint, metastable equilibria will be peaks in this probability landscape. One important feature of interest when studying noise-induced transitions is the optimal escape pathway from a metastable state or the optimal transition pathway from one metastable state to another. Of the many paths that lead to escape from a metastable state, or switching between two such states, there exists a most probable transition path. This path is known as the optimal escape or switching path. It is of great importance in a variety of applied problems to determine this optimal path since knowledge of the path then enables the determination of the mean time to escape from a metastable state or to switch from one metastable state to another.

While the noise that induces these rare transition events may be internal or external to the system, in this article, we only consider external noise. Mathematically, the effect of external noise is often

described using a Langevin equation or the associated Fokker–Planck equation (though the dynamics of external noise may sometimes be described by a master equation⁸). Feynman famously pointed out that each noise realization corresponds to a particular trajectory of the system, and, therefore, the probability density of realizations of trajectories is determined by the probability density of noise realizations.⁹ This idea can be used to formulate a variational problem to find the optimal path that ultimately reduces to considering trajectories of an auxiliary Hamiltonian dynamical system. One can solve for the Hamiltonian dynamics, either analytically or numerically, for the most probable (i.e., optimal) path of escape or switching.^{10,11}

The mean switching time (MST) essentially describes the dwell time of the system in a given basin of attraction, and as such, it is an important characteristic of the system. Accordingly, there has been an increased interest in the literature on using an external control to abate or enhance the mean switching time.^{6,12,13} However, the control strategies proposed in those works cannot control the switching time to a desired value. This is in part due to the difficulty of obtaining a closed form expression for the MST with fully described parameters, whose computation does not require experimentation or simulation. Such analytical expressions are only available for a very limited set of low-dimensional systems, e.g., escape from a one-dimensional potential well.¹⁴

In contrast, in the current work, we present a control strategy which uses limited control to achieve a desired MST. The strategy relies on knowledge about the basin boundaries of the region of attraction of the stable equilibrium of the deterministic system. These basin boundaries can be obtained using a variety of methods, including finite-time Lyapunov exponent (FTLE) computations.¹⁵ The required actuation for the strategy is minimal since the actual transition is precipitated by the noise in the system. We developed the approach in our previous work,¹⁶ where we exploited noise-driven transitions to control the dwell time of a marine robot operating in a gyre flow. In this work, we generalize the approach to a broader class of dynamical systems. The method enables one to control the MST of a stochastic dynamical system with metastable states to a desired value. To demonstrate the generality of the approach, we evaluate our method on two dynamical systems: (1) a double-gyre flow field and (2) a damped pendulum. The double-gyre flow is often used to model large scale circulations in the ocean,¹⁷ while the damped pendulum is representative of many practical dynamical systems, e.g., phase difference across a Josephson junction.¹⁸ To the best of our knowledge, this is the first attempt at using control to obtain a desired MST.

The rest of the article is organized as follows. In Sec. II, the background of the stochastic switching problem is presented while the effect of an external control field on the MST is analyzed in Sec. III. The proposed control strategy is presented in Sec. IV, and validation of the strategy for different systems is presented in Sec. V. The article contains concluding remarks in Sec. VI.

II. BACKGROUND

We consider a dynamical system that is affected by external noise. The system is modeled using the Langevin equation,

$$\dot{\mathbf{x}} = \mathbf{F}(\mathbf{x}) + \boldsymbol{\eta}(t), \tag{1}$$

where $\mathbf{x} \in \mathbb{R}^n$ is the state variable, \mathbf{F} is the nominal system, and $\boldsymbol{\eta}(t)$ is an uncorrelated white noise term where each component has zero mean and a standard deviation of $\sigma = \sqrt{2D}$, where D is the noise intensity. In (1), \mathbf{F} describes a deterministic nonlinear system with multiple equilibrium states. In addition to modeling errors, $\boldsymbol{\eta}(t)$ can also capture sensing, actuation, and environmental uncertainties. In the absence of noise, all trajectories of the system will approach the stable equilibrium states of the system. With the addition of external noise, the system trajectories will be governed by individual noise realizations. In fact, each realization of the noise $\boldsymbol{\eta}$ results in a corresponding trajectory of the state variable \mathbf{x} . The trajectories will now be concentrated around the metastable equilibria, and the probability density of the trajectories over the state space will have peaks near these equilibria (see Fig. 1). Even with infinitesimally small noise, there are rare noise-induced events in which the system transitions from one metastable state to another. The smaller the noise intensity, the larger the MST will be and vice versa.

Since each realization of the noise $\boldsymbol{\eta}$ results in a corresponding trajectory of the state variable \mathbf{x} , the probability of occurrence of a switch from one metastable state to another is governed by the probability of occurrence of the corresponding noise realization $\boldsymbol{\eta}(t)$.⁹ Of all the possible escape trajectories from a metastable state, there exists a trajectory that is probabilistically most likely to occur. It has been shown^{10,19} that the probability P of occurrence of a given noise trajectory is

$$P \propto e^{-R/D}, \tag{2}$$

where R is the action and is given as

$$R = \frac{1}{2} \int_{t_0}^{t_f} \boldsymbol{\eta}(t)^T \boldsymbol{\eta}(t) dt = \frac{1}{2} \int_{t_0}^{t_f} [\dot{\mathbf{x}} - \mathbf{F}(\mathbf{x})]^T [\dot{\mathbf{x}} - \mathbf{F}(\mathbf{x})] dt. \tag{3}$$

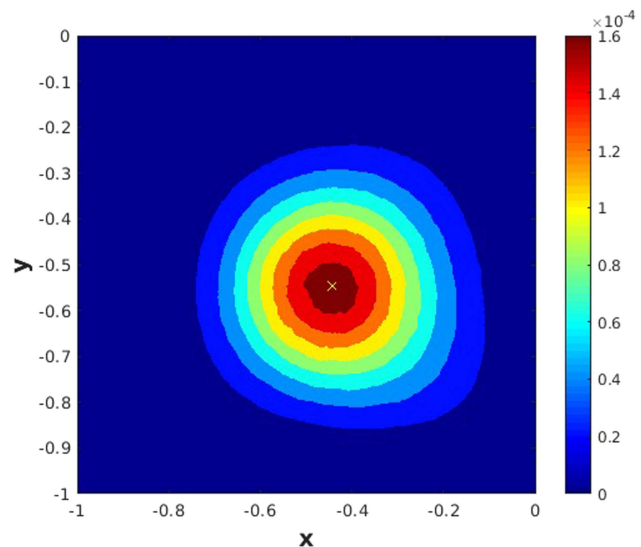


FIG. 1. Probability density of escape trajectories obtained from Monte Carlo simulations of the double-gyre flow given in (6) for parameters $A = 1$, $s = 1$, and $\mu = 1$. The equilibrium point (yellow cross) is now a peak in this probabilistic landscape.

Thus, the most probable switching path is the one with the minimum action given by

$$\mathcal{R} = \min_{\mathbf{x}(t)} \frac{1}{2} \int_{-\infty}^{\infty} [\dot{\mathbf{x}} - \mathbf{F}(\mathbf{x})]^T [\dot{\mathbf{x}} - \mathbf{F}(\mathbf{x})] dt. \quad (4)$$

Given an optimal path, (1) can be used to find the associated optimal noise realization. In the case of small noise, the switching rate is directly proportional to the probability of observing this optimal, or most probable, noise profile as all other noise realizations are exponentially less likely to occur.²⁰ The mean switching time (MST) can, therefore, be approximated by

$$T_E = be^{\mathcal{R}/D}, \quad (5)$$

where b is a prefactor determined through numerical simulation or an experiment. Figure 2(a) shows the phase portrait of a double-gyre

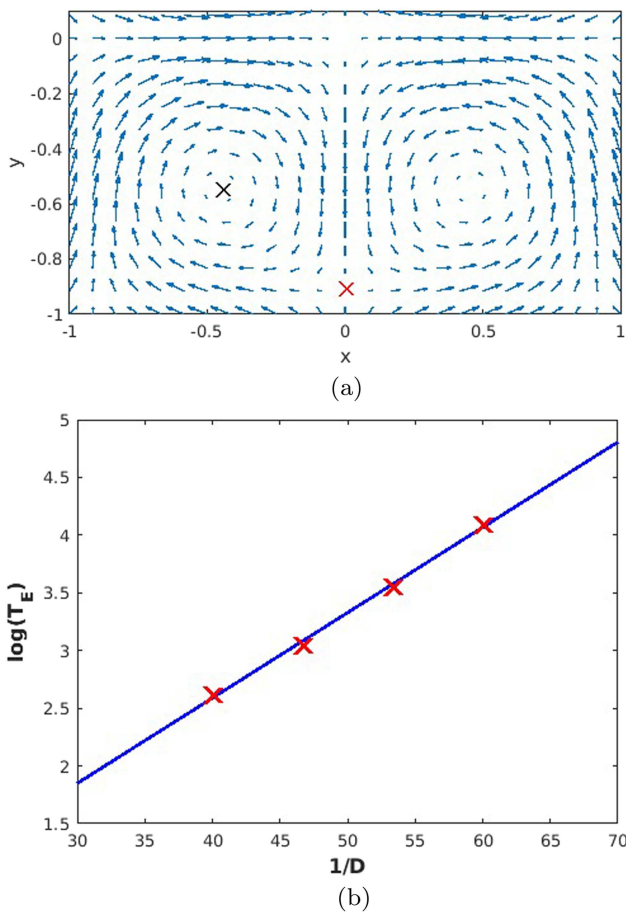


FIG. 2. (a) Phase portrait of the double-gyre flow for $A = 1$, $s = 1$, and $\mu = 1$. The black cross indicates the stable equilibrium at the center of the left gyre, and the red cross indicates the saddle point at the lower right corner; (b) Logarithm of the MST T_E vs $1/D$ for the double-gyre flow obtained using Monte Carlo simulations. The simulation results are consistent with the form of the theoretically predicted relationship between the MST and noise intensity given in (5). Red crosses are simulation data points, and the solid blue line is the line of best fit.

flow field given by

$$\mathbf{F}(x, y) = \begin{bmatrix} F_x(x, y) \\ F_y(x, y) \end{bmatrix} = \begin{bmatrix} -\pi A \sin(\frac{\pi x}{s}) \cos(\frac{\pi y}{s}) - \mu x \\ \pi A \cos(\frac{\pi x}{s}) \sin(\frac{\pi y}{s}) - \mu y \end{bmatrix}, \quad (6)$$

where A denotes the strength of the flow, s is a scaling factor for the gyre dimensions, and μ is a damping coefficient. Figure 2(b) shows the mean switching times obtained by performing Monte Carlo simulations for a range of noise intensities in this flow field for $A = 1$, $s = 1$, and $\mu = 1$. In these simulations, the system is initialized by placing a particle/sensor near the metastable state at the center of the left gyre. The particle will stay in the left gyre for a long period of time, but eventually the noise will cause the particle to undergo an escape event. The escape from the left gyre to the right gyre occurs when the particle transitions across the gyre boundary demarcated by the stable and unstable manifolds of the saddle points flanking each gyre. In Fig. 2(b), the crosses in red indicate simulation data points, and the solid line in blue indicates the line of best fit. It can be seen that the simulation results are consistent with the form of (5), and the intercept of this line of best fit allows us to obtain an estimate of the prefactor b . Figure 3 shows the switching path with the minimum action of noise, i.e., the optimal switching path or the most probable switching path (MPSP), overlaid on the probability density of simulated trajectories leading to escape for the double-gyre system. It can be seen that the theoretically predicted MPSP coincides with the peaks of the probability density function of the simulated escape trajectories. Figure 4 shows the MPSP for two dynamical systems: (1) the double-gyre system and (2) the damped pendulum. The arrows along the path indicate the strength and direction of the noise profile associated with this optimal path, and the basin boundaries are shown in red. It can be seen that the noise is similar to a control input that pushes the system toward the basin boundaries.

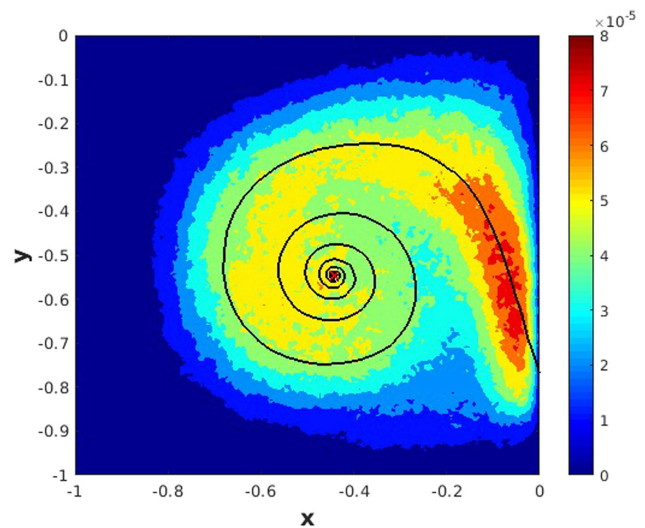


FIG. 3. The most probable switching path (MPSP) overlaid on the probability density of truncated escape trajectories obtained from Monte Carlo simulations of the double-gyre flow for parameters $A = 1$, $s = 1$, and $\mu = 1$. The paths were truncated to highlight the escape portion of the trajectories.

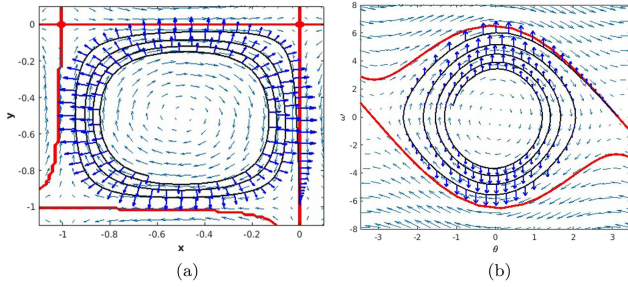


FIG. 4. The most probable switching path (the solid black curve) plotted on top of the phase portrait of (a) a double-gyre flow field and (b) a damped pendulum. The red line shows the boundary of the attracting region. The MPSP is computed from a stable equilibrium to one of the saddle points on the boundary, and it is truncated near the stable equilibrium for clarity. The optimal noise profile, shown in blue arrows along the MPSP, is directed toward the nearest boundary.

In the limit of small noise, each switching trajectory is a rare event, and, thus, the events are uncorrelated. Therefore, the switching events can be considered to be a Poisson process, and the probability density function of the mean switching times P_{T_E} is exponential with a mean switching time of T_E so that

$$P_{T_E}(t) = \frac{1}{T_E} e^{-\frac{t}{T_E}}, \quad t \geq 0. \quad (7)$$

III. STOCHASTIC TRANSITIONS WITH CONTROL

The central theme of this work is the control of the MST using an external control signal. The controlled system dynamics are given by

$$\dot{\mathbf{x}} = \mathbf{F}(\mathbf{x}) + \mathbf{u}(\mathbf{x}, t) + \boldsymbol{\eta}(t), \quad (8)$$

where \mathbf{u} is the control signal. Inspired by the noise profile associated with the optimal switching path (see Fig. 4), a control signal of the form $\mathbf{u} = c\mathbf{f}(\mathbf{x})$ is considered. The function $\mathbf{f}(\mathbf{x})$ gives the direction of the control with $\|\mathbf{f}(\mathbf{x})\| = 1$, and similar to the most probable noise profile, $\mathbf{f}(\mathbf{x})$ is selected to point toward the closest basin boundary. This form for the control law gives rise to a control signal which is similar to the optimal noise profile that leads to escape. Using (4), the action of the trajectory that is most likely to result in escape for this controlled system is given by

$$\mathcal{R}^c = \min_{\mathbf{x}^c(t)} \frac{1}{2} \int_{-\infty}^{\infty} [\dot{\mathbf{x}} - \mathbf{F}(\mathbf{x}) - c\mathbf{f}(\mathbf{x})]^T [\dot{\mathbf{x}} - \mathbf{F}(\mathbf{x}) - c\mathbf{f}(\mathbf{x})] dt. \quad (9)$$

Let the optimal switching path that is the solution to (9) be denoted by $\mathbf{x}^c(t)$. Thus, the action of the most likely noise profile can be rewritten as

$$\mathcal{R}^c = \frac{1}{2} \int_{-\infty}^{\infty} [\dot{\mathbf{x}}^c - \mathbf{F}(\mathbf{x}^c) - c\mathbf{f}(\mathbf{x}^c)]^T [\dot{\mathbf{x}}^c - \mathbf{F}(\mathbf{x}^c) - c\mathbf{f}(\mathbf{x}^c)] dt. \quad (10)$$

When $c = 0$, the action \mathcal{R}^0 is given by the solution to the uncontrolled case in (4), and the corresponding MPSP is $\mathbf{x}^0(t)$. Note that, for an arbitrary c , the optimal path $\mathbf{x}^c(t)$ depends on c . Using a Taylor

series expansion,

$$\mathbf{x}^c(t) = \mathbf{x}^0(t) + \left. \frac{\partial \mathbf{x}^c}{\partial c} \right|_{c=0} c + \mathcal{O}(c^2). \quad (11)$$

Thus, for small values of c such that the change in the optimal path is small, i.e., $\left| \frac{\partial \mathbf{x}^c}{\partial c} \right| \ll 1$, one has $\mathbf{x}^c(t) \approx \mathbf{x}^0(t)$. For small c , the action of the MPSP is, therefore, given by

$$\begin{aligned} \mathcal{R}^c &\approx \frac{1}{2} \int_{-\infty}^{\infty} [\dot{\mathbf{x}}^0 - \mathbf{F}(\mathbf{x}^0) - c\mathbf{f}(\mathbf{x}^0)]^T [\dot{\mathbf{x}}^0 - \mathbf{F}(\mathbf{x}^0) - c\mathbf{f}(\mathbf{x}^0)] dt \\ &\approx \frac{1}{2} \int_{-\infty}^{\infty} [\dot{\mathbf{x}}^0 - \mathbf{F}(\mathbf{x}^0)]^T [\dot{\mathbf{x}}^0 - \mathbf{F}(\mathbf{x}^0)] dt \\ &\quad - c \int_{-\infty}^{\infty} \mathbf{f}(\mathbf{x}^0)^T [\dot{\mathbf{x}}^0 - \mathbf{F}(\mathbf{x}^0)] dt \\ &= \mathcal{R}^0 - c \int_{-\infty}^{\infty} \mathbf{f}(\mathbf{x}^0)^T \boldsymbol{\eta}^0(t) dt. \end{aligned}$$

This can be written concisely as

$$\mathcal{R}^c \approx \mathcal{R}^0 - \alpha c, \quad (12)$$

where

$$\alpha = \int_{-\infty}^{\infty} \mathbf{f}(\mathbf{x}^0)^T \boldsymbol{\eta}^0(t) dt$$

and $\boldsymbol{\eta}^0(t)$ is the optimal noise profile for the uncontrolled case. Note that similar to $\boldsymbol{\eta}^0$, $\mathbf{f}(\mathbf{x})$ is always directed toward the basin boundary, and as such $\mathbf{f}(\mathbf{x}^0) \approx \frac{\boldsymbol{\eta}^0}{|\boldsymbol{\eta}^0(t)|}$, i.e., $\mathbf{f}(\mathbf{x}^0)$ and $\boldsymbol{\eta}^0$ are approximately parallel. In addition, $\lim_{t \rightarrow \pm\infty} \boldsymbol{\eta}^0(t) = 0$. Thus, $0 < \alpha < \infty$, and the change in the action due to the external control field is

$$\Delta \mathcal{R} = -\alpha c. \quad (13)$$

Using (5), the change in the mean switching time due to this change in the action is given by

$$\frac{T_E^c}{T_E^0} = e^{\Delta \mathcal{R}/D}, \quad (14)$$

where T_E^c and T_E^0 are the MST for the controlled and uncontrolled cases, respectively. From (13) and (14), it can be seen that $c < 0$ implies $T_E^c > T_E^0$. Similarly, $c > 0$ implies $T_E^c < T_E^0$. Thus, it is evident that the MST of a system can be changed using an external control signal of the suggested form. If the dynamical system and the noise in the system are completely known, (14) can be used to compute the external control required to achieve a desired MST. However, in practical systems, these details are often unknown. The synthesis of a control strategy to obtain a desired MST, in cases where the details about the dynamical system and/or the noise in the system are not fully known, is presented in Sec. IV.

IV. CONTROL STRATEGY

From (5), it can be seen the average time required to escape from one attractor depends on the action as well as the amount of noise in the system. For a given noise intensity, the MST is governed by the action of the transition path that is most likely to occur. The objective of this work is to use a control of the form $\mathbf{u} = c\mathbf{f}(\mathbf{x})$, in which the

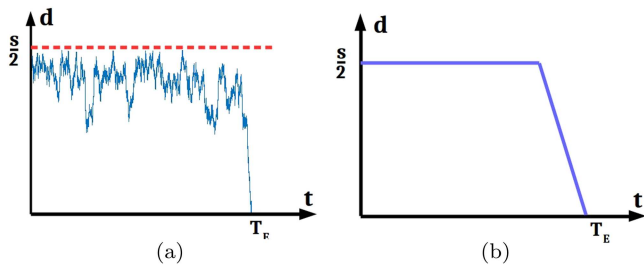


FIG. 5. (a) Variation of the distance to the closest gyre boundary over time along a noise-driven switching trajectory in a double-gyre system. The width of the attracting region is s . The red dashed line indicates the distance to the boundary from the gyre center. (b) The switching trajectory hovers near the stable equilibrium before exhibiting an almost linear transition toward escape.

parameter $c \in [-c_{max}, c_{max}]$ can be varied to obtain a desired MST, T_E^d , by changing the action. Since $\|f(x)\| = 1$, c_{max} corresponds to the maximum available control authority.

If the noise intensity D , the current MST T_E^0 , and the dynamics of the system are fully known, then (13) and (14) can be used to compute the value of c required to obtain a desired MST. Typically, most of this information is not readily available in a real system. Thus, to design a control strategy to obtain the desired MST, we must first understand the characteristic behavior of a noise-driven switching trajectory in a dynamical system with multiple stable states. Figure 5(a) shows the typical variation of the distance d between a point on a trajectory and the closest basin boundary over time, until escape from the attracting region through one of the basin boundaries occurs. A simplified d vs t plot that captures the essential characteristic of the curve in Fig. 5(a) is shown in Fig. 5(b). Although Fig. 5(a) is generated using a trajectory realization obtained from a double-gyre flow field, this type of variation for the distance to boundary is typical of switching trajectories in general multistable dynamical systems. A major portion of the system trajectory is concentrated around the stable equilibrium, before it suddenly transitions out of the attracting region. The actual transition itself occurs over a fraction of the overall dwell time, and near the transition, the d vs t curve is approximately linear. These

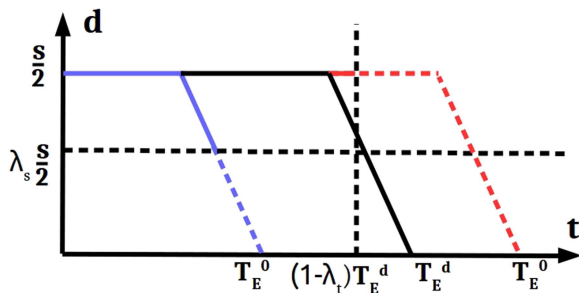


FIG. 6. Desired noise-driven switching trajectory with a desired MST of T_E^d (black); actual switching trajectory when $T_E^0 < T_E^d$ (blue); and actual switching trajectory when $T_E^0 > T_E^d$ (red). The parameters λ_s and λ_t are used to determine the regions R_1 , R_2 , and R_3 as described in the text and shown in Fig. 7.

typical characteristics can be used to identify a potential onset of the escape portion of a trajectory, when neither the noise level of the system nor the MSTs are known.

A. Controller synthesis

Let T_E^0 be the “natural” MST of the uncontrolled system for an unknown noise level, and let T_E^d be the desired MST. If the noise in the system is high, then $T_E^0 < T_E^d$ (blue trace in Fig. 6), and if the noise in the system is low, then $T_E^0 > T_E^d$ (red trace in Fig. 6). Note that T_E^0 of the system is unknown. The proposed control strategy selects values for c depending on the region of the d vs t curve in which the system is operating at any given time. The three regions, shown in Fig. 7, are given by

$$R_1 = \{(t, d) \mid 0 < t < (1 - \lambda_t)T_E^d, 0 < d \leq \lambda_s s/2\},$$

$$R_2 = \{(t, d) \mid t \geq (1 - \lambda_t)T_E^d\},$$

$$R_3 = \{(t, d) \mid 0 < t < (1 - \lambda_t)T_E^d, d > \lambda_s s/2\},$$

where λ_t and λ_s are parameters which define the region boundaries.

If $(t, d) \in R_1$ (e.g., dashed portion of the blue trace in Fig. 6), the system’s trajectory is too close to the basin boundary before the required time has elapsed. According to the simplified d vs t characteristic curve shown in Fig. 5(b), it is assumed that this is indicative of the onset of a switching event. Assuming a linear behavior along the escape portion of the trajectory, an estimate for the current uncontrolled MST can be computed to be

$$T_E^0 = \frac{t}{1 - \lambda_t \frac{2d}{\lambda_s s}}. \tag{15}$$

Using (14), the required change in action to obtain the desired MST can be approximated as

$$\Delta \mathcal{R} = k \log \left(\frac{T_E^d}{T_E^0} \right),$$

where k is a user defined parameter which governs how aggressive the control is. Using (13), the control parameter c is set to be

$$c = \max \left(-\frac{\Delta \mathcal{R}}{\alpha}, -c_{max} \right). \tag{16}$$

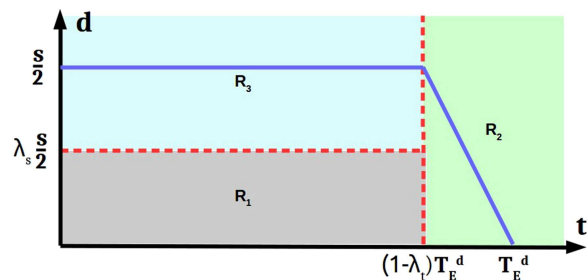


FIG. 7. The regions of operation used to determine the direction and strength of the external control field.

When $(t, d) \in R_2$ (e.g., dashed portion of the red trace in Fig. 6), it is assumed that $T_E^0 \geq T_E^d$ and that the particle has not started its transition toward escape. In contrast to the previous case, an estimate for T_E^0 cannot be obtained. Furthermore, in order to meet the desired MST target, the particle must transition out as soon as possible. In this case, the control parameter is set as

$$c = c_{max}.$$

Therefore, the proposed control strategy is based on making local assumptions about T_E^0 and is given by $\mathbf{u} = \mathbf{c}\mathbf{f}(\mathbf{x})$, where c is defined as

$$c = \begin{cases} \max\left(-\frac{\Delta \mathcal{R}}{\alpha}, -c_{max}\right) & (t, d) \in R_1, \\ c_{max} & (t, d) \in R_2, \\ 0 & (t, d) \in R_3, \end{cases} \quad (17)$$

and as shown in Sec. III, $\mathbf{f}(\mathbf{x})$ is a unit vector pointed toward the closest basin boundary.

Essentially, the control strategy pushes the agent away from the basin boundary if it gets close to the boundary before the required amount of time has elapsed, and it pushes the agent toward the boundary when the elapsed time is close to the required MST. The instances at which the control is switched on are governed by the parameters λ_s and λ_t . Note that $\lambda_t \leq 1$ and $0 \leq \lambda_s \leq 1$. Intuitively, it can be seen that large values of λ_s will increase the MST and that large values of λ_t will decrease the MST.

B. Analysis of the control strategy

In order to analyze the proposed control strategy and verify its correctness, the strategy is analyzed using a 1D system. This greatly simplifies the analysis while preserving the essential characteristics of the controlled system. Insights from the 1D system are then used to select values for λ_s and λ_t . Consider a particle in a 1D potential well, subject to Gaussian noise. The equation of motion of this particle is given by

$$\dot{x} = -\frac{\partial U}{\partial x} + \eta(t) + u(t), \quad (18)$$

where x is the position, U represents the potential well (see Fig. 8), $u(t)$ is the control, and η is Gaussian noise with intensity D . For the uncontrolled case, i.e., $u(t) = 0$, it has been shown²¹⁻²³ that if $\Delta U/D \gg 1$, the average time T_E required for a particle to escape the stable equilibrium at x_{min} is given by

$$T_E^0 = \frac{1}{D} \int_{x_1}^{x_2} e^{-\left(\frac{U_{min}}{D} + \frac{U''_{min}}{2D}(x-x_{min})^2\right)} dx \times \int_{x_{min}}^A e^{\left(\frac{U_{max}}{D} - \frac{|U''_{max}|}{2D}(x-x_{max})^2\right)} dx, \quad (19)$$

where U''_{min} and U''_{max} are the second derivatives of $U(x)$ at x_{min} and x_{max} , respectively, and A is a point away from x_{max} as shown in Fig. 8. Further details of this derivation can be found in a recent review article.²³ Considering the exponential fall off of the integrands and extending the limits of both integrals from $-\infty$ to ∞ , one can show

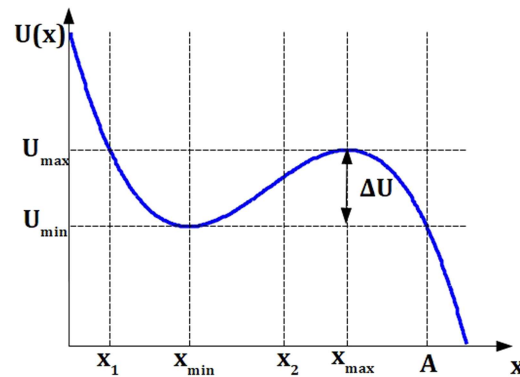


FIG. 8. Potential well $U(x)$.

that

$$T_E^0 = \frac{2\pi}{\sqrt{|U''_{min}| |U''_{max}|}} e^{\frac{\Delta U}{D}}. \quad (20)$$

This is the well known Kramers' escape rate for 1D systems.¹⁴

Now consider a control of $u(t) = c \frac{\partial U}{\partial x}$ with $|c| \leq c_{max} < 1$. Such a control results in a controlled 1D system given by

$$\dot{x} = -(1-c) \frac{\partial U}{\partial x} + \eta(t). \quad (21)$$

This is equivalent to considering a potential well $\hat{U} = (1-c)U$. Thus, for $c < 0$, the well becomes deeper and for $0 < c < 1$, the well becomes shallower. Substituting $U = \hat{U}$ in (19) and (20), one obtains

$$T_E^c = \frac{2\pi}{(1-c)\sqrt{|U''_{min}| |U''_{max}|}} e^{(1-c)\frac{\Delta U}{D}} = \frac{e^{-c\frac{\Delta U}{D}}}{1-c} T_E^0. \quad (22)$$

It can be shown that $c < 0 \Rightarrow T_E^c > T_E^0$, and $0 < c < 1 \Rightarrow T_E^c < T_E^0$ when $\Delta U/D \gg 1$, i.e., $c > 0$ pushes the particle out toward the boundary and $c < 0$ pulls the particle in toward the center of the well.

The corresponding region based control strategy for c as proposed in (17) is given by

$$c = \begin{cases} < 0, & x_s \leq x < x_{max} \text{ and } t < T_t, \\ > 0, & t \geq T_t, \\ = 0 & \text{otherwise,} \end{cases} \quad (23)$$

where $x_s = x_{max} - \lambda_s(x_{max} - x_{min})$ and $T_t = (1 - \lambda_t)T_E^d$, with $\lambda_t \leq 1$ and $0 \leq \lambda_s \leq 1$. In the remainder of this section, we show that this region based controller is able to achieve any desired MST within bounds that are dependent on the maximum available control.

To obtain an expression for the MST under the proposed control strategy, first consider applying a control with $c < 0$ for $x_s \leq x < x_{max}$, without considering the elapsed time [case 1 of the control strategy in (23)]. In this case, the control action can be written as $u(t) = -|c|(\Theta(x - x_s) - \Theta(x - x_{max})) \frac{\partial U}{\partial x}$, where Θ is a Heaviside

function. Thus, the first integral I_1 of (19) for the mean escape time can now be written as

$$I_1 = \int_{x_1}^{x_s} e^{-\left(\frac{U_{min}}{D} + \frac{U''_{min}}{2D}(x-x_{min})^2\right)} dx + \int_{x_s}^{x_2} e^{-(1+|c|)\left(\frac{U_{min}}{D} + \frac{U''_{min}}{2D}(x-x_{min})^2\right)} dx. \tag{24}$$

Considering that the integrands of both integrals decay exponentially, the lower limit of the first integral can be extended to $-\infty$, and the upper limit of the second integral can be extended to ∞ . Thus,

$$I_1 = \sqrt{\frac{\pi D}{2U''_{min}}} e^{-\frac{U_{min}}{D}} \left(1 + \operatorname{erf}\left(\sqrt{\frac{U''_{min}}{2D}}(x_s - x_{min})\right) + \frac{e^{-\frac{|c|U_{min}}{D}}}{\sqrt{1+|c|}} \left(1 - \operatorname{erf}\left(\sqrt{\frac{(1+|c|)U''_{min}}{2D}}(x_s - x_{min})\right) \right) \right). \tag{25}$$

Using similar arguments, the second integral I_2 of (19) can be written as

$$I_2 = \sqrt{\frac{\pi D}{2|U''_{max}|}} e^{\frac{U_{max}}{D}} \left(2 + \operatorname{erf}\left(\sqrt{\frac{U''_{max}}{2D}}(x_s - x_{max})\right) - \frac{e^{\frac{|c|U_{max}}{D}}}{\sqrt{1+|c|}} \operatorname{erf}\left(\sqrt{\frac{(1+|c|)U''_{max}}{2D}}(x_s - x_{max})\right) \right). \tag{26}$$

In (25) and (26), $\operatorname{erf}(x) = \frac{2}{\sqrt{\pi}} \int_0^x e^{-t^2} dt$. Thus, the expected MST, when control of $c < 0$ is enacted for $x_s \leq x < x_{max}$, is

$$T_{E,dist}^c = \frac{1}{D} I_1 I_2. \tag{27}$$

Next, consider introducing a control with $c > 0$ when $t \geq T_t$. Due to the stochastic nature of escape events, of the total paths that escape, $\int_0^{T_t} P_{T_E}(t) dt$ of them would have already escaped before the $c > 0$ control is switched on at $t = T_t$. Recalling (7), we know that $P_{T_E}(t)$ is the probability distribution of the escape times before switching on the $c > 0$ control, and it is exponentially distributed, i.e., $P_{T_E}(t) = \frac{1}{T_{E,dist}^c} e^{-\frac{t}{T_{E,dist}^c}}$. Thus, the percentage of particles escaping

after turning on the $c > 0$ control is $1 - \int_0^{T_t} P_{T_E}(t) dt$, and the mean escape time for these particles is $T_t + T_E^c$, where T_E^c is the mean escape time if the $c > 0$ control is applied $\forall t \geq 0$, and is given by (22). Thus, the expected mean switching time under the full control strategy proposed in (23) is

$$T_E^{exp} = \int_0^{T_t} t P_{T_E}(t) dt + (T_t + T_E^c) \left(1 - \int_0^{T_t} P_{T_E}(t) dt \right).$$

Using (7), this can be simplified as

$$T_E^{exp} = T_{E,dist}^c - (T_{E,dist}^c - T_E^c) e^{-\frac{(1-\lambda_t)T_t}{T_{E,dist}^c}}, \tag{28}$$

where $T_{E,dist}^c$ is given in (27) and T_E^c is the nominal mean switching time if a control of $c > 0$ is used $\forall t \geq 0$. Note that we have also used the fact that $T_t = (1 - \lambda_t) T_E^d$, where T_E^d is the desired MST.

For $c = 0$, it is trivial to see that $T_E^c = T_{E,dist}^c = T_E^0$. It can be shown that for $\Delta U/D \gg 1$, $\partial T_{E,dist}^c / \partial |c| > 0$ and $\partial T_E^c / \partial c < 0$. Thus, it can be inferred that $T_{E,dist}^c \geq T_E^c$, with equality at the trivial case of $c = 0$. Using this, one can easily show that $\frac{\partial T_E^{exp}}{\partial \lambda_t} < 0$ and is continuous for $\lambda_t \leq 1$. Thus, T_E^{exp} is minimized at $\lambda = 1$ and it is maximized as $\lambda_t \rightarrow -\infty$. Thus, from (28), it can be seen that

$$T_E^c \leq T_E^{exp} < T_{E,dist}^c, \tag{29}$$

with $T_E^{exp} = T_E^c$ for $\lambda_t = 1$ and $T_E^{exp} \rightarrow T_{E,dist}^c$ for $\lambda_t \rightarrow -\infty$. Thus, for a given c and λ_s , there exists $\lambda_t \leq 1$ that can achieve a desired escape time in the range established in (29).

As mentioned before, it can be shown that for $\Delta U/D \gg 1$, $\partial T_{E,dist}^c / \partial |c| > 0$ and $\partial T_{E,dist}^c / \partial \lambda_s > 0$. In addition, $T_{E,dist}^c|_{c=0} = T_E^0$ and $T_{E,dist}^c|_{\lambda_s=0} = T_E^0$. Thus, the maximum of $T_{E,dist}^c$ occurs at $c = -c_{max}$ and $\lambda_s = 1$. Substituting these values in (27), we have

$$T_E^0 \leq T_{E,dist}^c \leq T_{max}, \tag{30}$$

where

$$T_{max} = \frac{T_E^0}{4} \left(1 + \frac{e^{-c_{max} \frac{U_{min}}{D}}}{\sqrt{1+c_{max}}} \right) \left(1 + \frac{e^{c_{max} \frac{U_{max}}{D}}}{\sqrt{1+c_{max}}} \right).$$

Thus, there exists a $(-c_{max} \leq c \leq 0, 0 \leq \lambda_s \leq 1)$ tuple that can achieve any $T_{E,dist}^c$ value in the range given in (30).

In a similar fashion, one can show that there exists a $0 \leq c \leq c_{max}$ that can achieve any T_E^c value in the range,

$$T_{min} \leq T_E^c \leq T_E^0,$$

where

$$T_{min} = \frac{e^{-c_{max} \frac{\Delta U}{D}}}{1 - c_{max}} T_E^0.$$

From the above observations, it can be concluded that there exist $-c_{max} \leq c \leq c_{max}$, $\lambda_t \leq 1$, and $0 \leq \lambda_s \leq 1$ that can achieve any desired mean switching time in the range $T_{min} \leq T_E^d < T_{max}$.

It is worth noting that for the above controller, $c < 1$ was considered in the analysis. If $c > 1$, the peak and the trough of the effective potential $(1 - c)U$ will be swapped, and the $\Delta U/D \gg 1$ assumption would not hold anymore.

C. Controller parameter selection in for general systems

If T_E^d lies between the T_{min} and T_{max} limits specified previously, there always exists a set of $(c, \lambda_t, \lambda_s)$ values that will achieve the desired MST. If the noise intensity D is known, depending on T_E^d , a suitable set of $(c, \lambda_t, \lambda_s)$ values can be selected to achieve T_E^d . In general, the noise level D is not known. In such cases, not only is it impossible to determine a set of $(c, \lambda_t, \lambda_s)$ values to achieve a given T_E^d but it is also not possible to determine if the required T_E^d value is even feasible. In a general higher-dimensional system, selecting a set of $(c, \lambda_t, \lambda_s)$ is even more complicated since an expression for T_E of the form given in (22) is not available.

In the control strategy given in Sec. IV A, the problems outlined above are overcome by first selecting values for c, λ_t, λ_s that approximately achieve the desired MST for $T_E^d > T_E^0$ and then by refining

λ_t to achieve T_E^d when $T_E^d < T_E^0$. For the $T_E^d > T_E^0$ case, the current uncontrolled MST T_E^0 is approximately estimated using (15) and then a value for c that would make $T_E \rightarrow T_E^d$ is selected using $c < 0$ control alone. Note that for this T_E to be achieved using $c < 0$ control alone, $\lambda_s = 1$. Thus, for this case, $T_{E,dist}^c \approx T_E^d$. According to (28), to make $T_E^{exp} \approx T_{E,dist}^c \approx T_E^d$, we need $\lambda_t \rightarrow -\infty$. That is, by selecting a large value for λ_s and a large negative value for λ_t , we are able to approximately achieve T_E^d if $T_E^d > T_E^0$. However, if $T_E^d < T_E^0$, this large negative value for λ_t will not be able to achieve the required T_E^d . Thus, in order to achieve the desired MST for both $T_E^d > T_E^0$ and $T_E^d < T_E^0$, we select $0 \ll \lambda_s < 1$ and $0 < \lambda_t \ll 1$, i.e., λ_s close to 1, and λ_t close to zero.

V. RESULTS

The control strategy given in Sec. IV A was used to control the mean switching time to a desired value in two dynamical systems exhibiting multiple stable equilibria, the double-gyre flow model and the damped pendulum model. In all of the following simulations, the Euler–Maruyama method was used for integrating the stochastic differential equations.

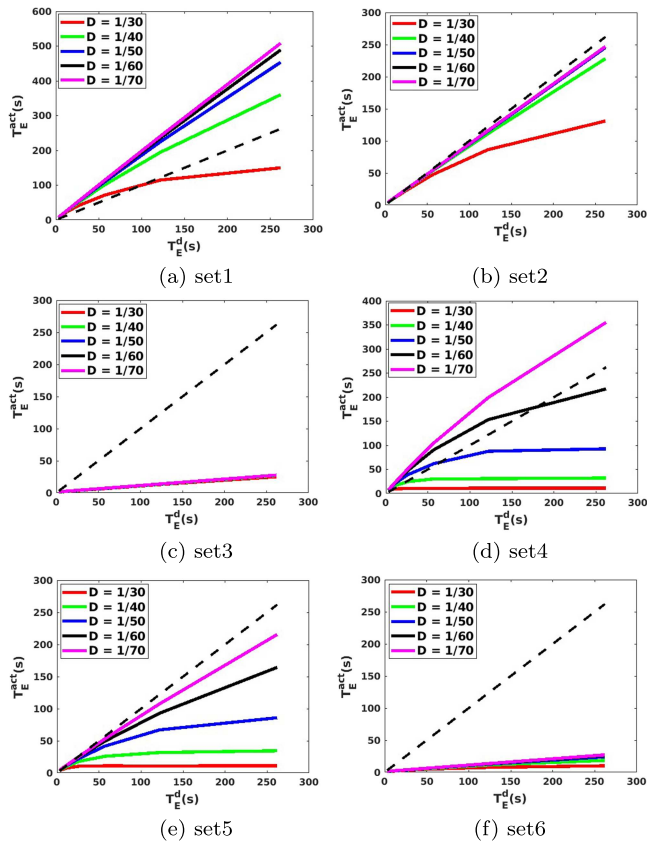


FIG. 9. Desired MSTs T_E^d vs the actual MSTs T_E^{act} for different (λ_s, λ_t) value combinations. The values of λ_s and λ_t for each set is given in Table I.

TABLE I. Values of λ_s and λ_t used in the simulations.

	Set 1	Set 2	Set 3	Set 4	Set 5	Set 6
λ_s	0.85	0.85	0.85	0.2	0.2	0.2
λ_t	-1	0.0625	0.9	-1	0.0625	0.9

A. Simulation results for a double-gyre flow

The double-gyre flow model is often used to describe large scale recirculation in the ocean,¹⁷ and it is given in (6). Figure 2(a) shows the phase portrait of the flow for $A = 1, s = 1$, and $\mu = 1$. For $\mu > 0$, each gyre has a deterministic attractor in the center of the gyre and is flanked by four saddle points. The gyre boundaries consist of the stable and unstable manifolds of these saddle points. A system of two adjoining gyres as shown in Fig. 2(a), qualitatively resembles a double-well potential.

Using the same parameter values ($A = 1, \mu = 1$ and $s = 1$), the stochastic double-gyre was considered in the simulations, with noise intensities given in the set $D = \{1/30, 1/40, 1/50, 1/60, 1/70\}$. For each noise intensity, a set of desired MSTs given by $T_E^d = \{3, 6, 12, 26, 57, 122, 262\}$ were considered. These T_E^d values approximately correspond to the natural mean switching times T_E^0 for noise intensities $\{1/20, 1/30, 1/40, 1/50, 1/60, 1/70, 1/80\}$, respectively. For each (D, T_E^d) pair, 1000 simulation trials, each starting near the center of the left gyre, were conducted. Each simulation trial was terminated when the system state escaped the boundaries of the left gyre. In all simulations, $c_{max} = 0.5$ was considered. In order to investigate the effect of selecting different λ_s and λ_t values, simulations were run for the (λ_s, λ_t) value combinations given in Table I. In sets 1–3, a large value is selected for λ_s (≈ 1), and in sets 4–6, a small value is selected for λ_s . In both cases, λ_t is successively increased from a

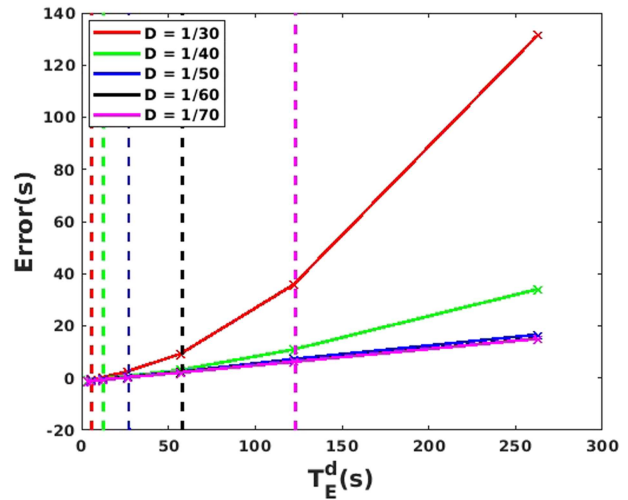


FIG. 10. Error $E = T_E^d - T_E^{act}$ vs T_E^d curves for different noise levels in the system. The vertical dashed lines represent the uncontrolled MST for each noise level.

negative value toward 1. From the discussion in Sec. IV C, the best results should be expected for set 2, where λ_s is large and λ_t is moderate. Figures 9(a)–9(f) show plots of desired MST, T_E^d , vs the actual MST, T_E^{act} , for different (λ_s, λ_t) value combinations. For each set of (λ_s, λ_t) values, multiple noise levels are considered. In each figure, the thick dotted line in black represents the ideal $T_E^d = T_E^{act}$ curve. The closer the T_E^d vs T_E^{act} curves are to this line, the better the performance of the control strategy.

Figures 9(a)–9(f) show that set 2 ($\lambda_s = 0.85, \lambda_t = 0.0625$), indeed gives the best results. In set 1, T_E^{act} overshoots T_E^d by a considerable margin since the negative value used for λ_t cannot pull back $T_{E_{dist}}^c$ in (28) enough toward $T_{E^c}^c$. On the other hand, in set 3, where λ_t is close to 1, $T_{E_{dist}}^c$ is pulled too far back by the $c > 0$ control, which results in very small T_E^{act} values. Set 4 and set 6 follow similar behaviors as set 1 and set 3, respectively, due to the effect of λ_t . While sets 2 and 5 consider the same moderate value for λ_t , in set 5, T_E^{act} undershoots T_E^d due to the small value of λ_s considered in set 5. Note that even in set 2, which has the best performance, large desired MSTs cannot be obtained when the noise in the system is high [see red line in Fig. 9(b)]. In such cases, the available control is not sufficient to achieve MSTs which are much greater than the “natural” MST of the system. In these cases, the desired MST falls outside the established limits.

Figure 10 shows the error $E = T_E^d - T_E^{act}$, for set 2 in Table I ($\lambda_s = 0.85$ and $\lambda_t = 0.0625$), which has the best performance among the parameter values tested. The error is plotted against the desired MST for a collection of noise levels in the system. The vertical dashed lines represent the “natural” MSTs for each noise level. It can be seen that the errors are well contained even when the desired MSTs are much higher than the “natural” MSTs. For noise level $D = 1/30$, the available control is insufficient to overcome the noise for large T_E^d values.

Figures 11(a)–11(f) show the probability densities of the MSTs obtained for different values of T_E^d . For these simulations, a noise level of $D = 1/60$, which has a “natural” MST of approximately 57 s, was considered. We used $\lambda_s = 0.85$ and $\lambda_t = 0.0625$ for the control. It can be seen that the proposed control is able to achieve T_E^d values that are much farther away from the natural MST. From these results, it can be seen that the control strategy proposed in Sec. IV A is able to achieve a wide range of desired MSTs, for a wide range of system noise levels.

The control strategy was also tested with a non-Gaussian noise source to check its performance in a nonideal scenario. In this case, the noise signal was derived as $\eta(t) = \tilde{\sigma} z^{1/3}(t) + \delta$, where each component of \mathbf{z} has a standard normal distribution, i.e., $z_i \sim \mathcal{N}(0, 1)$. The value for $\tilde{\sigma}$ was selected so that the standard deviation of each component of η was equal to the standard deviations considered in the Gaussian case, i.e., $\sigma(\eta_i) = \sqrt{2D}$ for $i = 1, 2$. As each component of the mean δ is the same value δ , this term essentially shifts the flow velocities in (1) by a constant amount, and its value is selected to be small enough such that the gyre structure of the flow is maintained. Figure 12 shows the results for the case where $\delta = 0.1$, $\lambda_s = 0.85$, and $\lambda_t = 0.0625$. In the cases shown, $\tilde{\sigma}$ was selected such that the noise signals have the same standard deviations as before. It can be seen that the desired MSTs are achieved with relatively small errors, even in the presence of non-Gaussian noise sources. Comparing the error curves for the Gaussian and non-Gaussian cases,

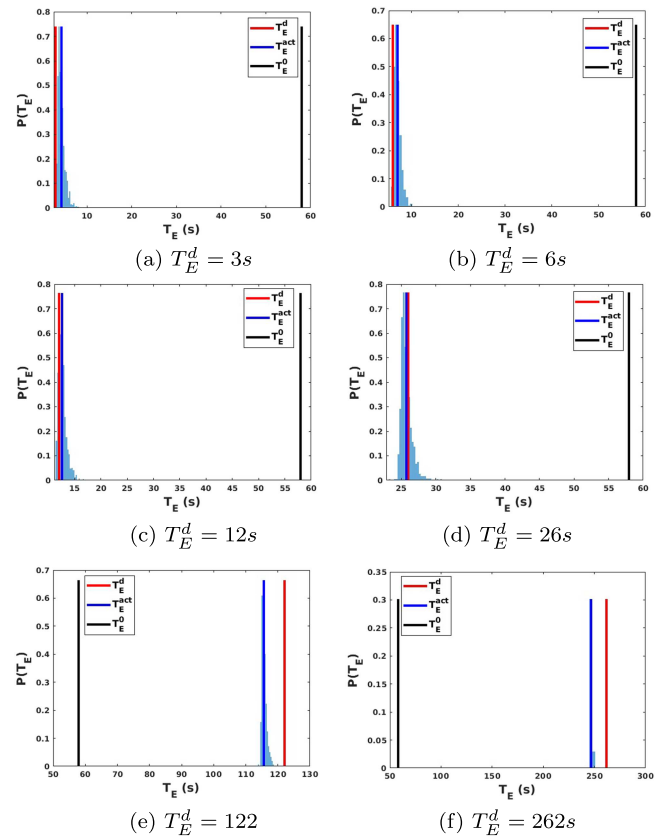


FIG. 11. Probability density function of the actual MSTs for various values T_E^d for a noise level of $D = 1/60$, where $\lambda_s = 0.85$ and $\lambda_t = 0.0625$ were used for the control.

it can be seen that the performance is only slightly degraded in the non-Gaussian case.

B. Simulation results for a damped pendulum

The proposed control method was used to control the MST in a damped pendulum system given by

$$\ddot{\theta} = -\frac{g}{L} \sin \theta - \beta \dot{\theta} + u, \tag{31}$$

where θ is the angle measured anticlockwise from the downward direction, g is the gravitational constant, L is the length of the pendulum, β is the damping coefficient, and u is the external control force. Considering the state space representation of this system, the noise-affected system can be expressed in the form of (8), where

$$\mathbf{F}(\mathbf{x}) = \begin{bmatrix} \omega \\ -\frac{g}{L} \sin \theta - \beta \omega \end{bmatrix}, \tag{32}$$

with state $\mathbf{x} = [\theta, \omega]^T$, control $\mathbf{u} = [0, u]^T$, and noise $\boldsymbol{\eta} = [0, \eta]^T$. Note that 1D control and noise fields are considered since the original system only has a 1D control.

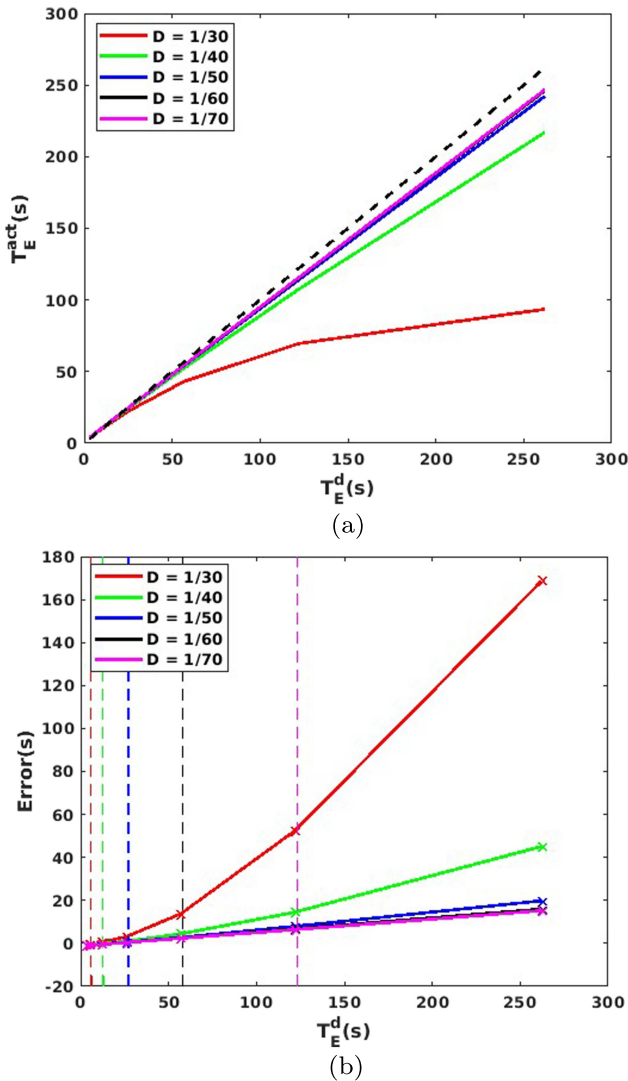


FIG. 12. Simulation results for non-Gaussian noise, where $\eta(t) = \tilde{\sigma} \mathbf{z}^{1/3}(t) + \delta$ with $\delta = 0.1$, $\lambda_s = 0.85$, and $\lambda_t = 0.0625$, and where $\tilde{\sigma}$ was selected such that $\sigma(\eta_i) = \sqrt{2D}$ for $i = 1, 2$. (a) T_E^d vs T_E^{act} curves for different noise levels and (b) error $E = T_E^d - T_E^{act}$ vs T_E^d curves for different noise levels.

A damped pendulum with parameters $L = 1$ and $\beta = 0.1253$ was considered in the simulations (see Fig. 13). Noise intensities in the set $D = \{1/3, 1/2, 1\}$ were used in the simulations, and for each noise intensity, a set of desired MSTs given by $T_E^d = \{1778, 254, 45, 25\}$ were considered. These T_E^d values approximately correspond to the natural mean switching times T_E^0 for noise levels $\{1/3, 1/2, 1, 1.5\}$, respectively. For each (D, T_E^d) pair, 1000 trials were simulated until escape through the basin boundary (the basin boundary is shown by the black line in Fig. 13). As proposed in Sec. IV C, a large value was selected for λ_s and a small value was selected for λ_t . Figure 14 shows the desired MST T_E^d vs the actual MST T_E^{act} for

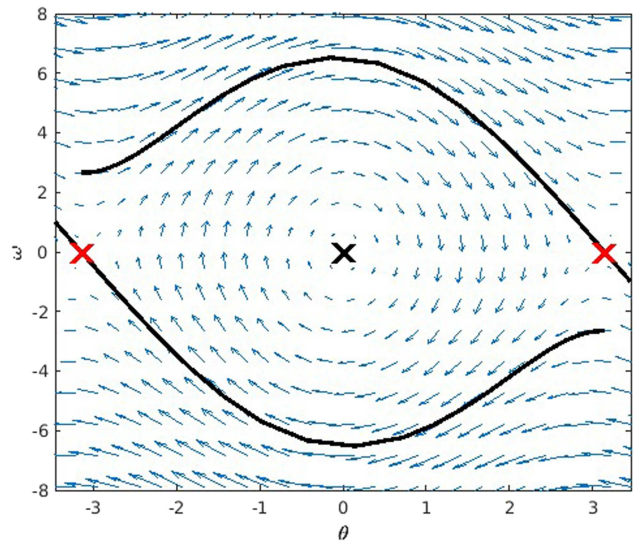


FIG. 13. Phase portrait for the damped pendulum system given in (31) for $L = 1$ and $\beta = 0.1253$. The deterministically stable equilibrium is shown by the black cross, and the two saddle points are shown by red crosses.

different noise intensities with $\lambda_s = 0.9$ and $\lambda_t = 0.01$. It can be seen that the proposed external control is able to achieve MSTs that are much different to the natural uncontrolled switching time of the system. Figure 15 shows the error $E = T_E^d - T_E^{act}$, for parameter values $\lambda_s = 0.9$ and $\lambda_t = 0.01$. Similar to the double-gyre system, the errors are well contained even when the desired MSTs are much different from the “natural” MSTs.

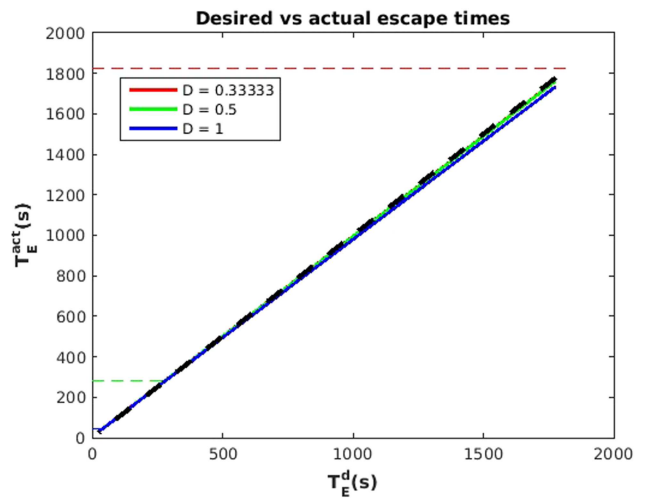


FIG. 14. Desired MSTs T_E^d vs the actual MSTs T_E^{act} for different noise intensities with $\lambda_s = 0.9$ and $\lambda_t = 0.01$ for the damped pendulum. The colored horizontal dashed lines indicate the “natural” uncontrolled MST for each noise level.

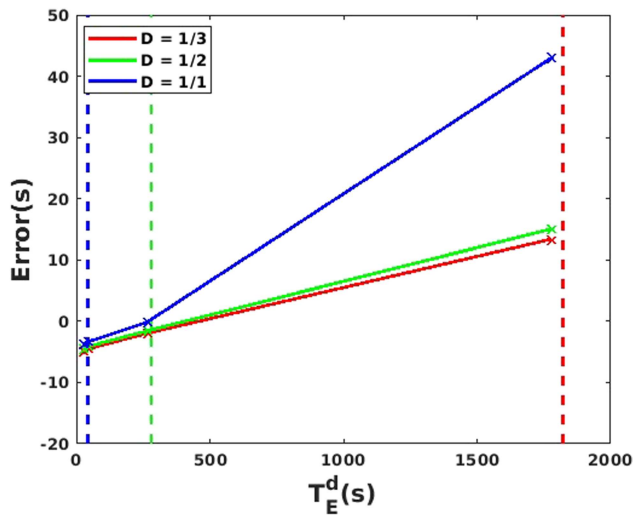


FIG. 15. Error $E = T_E^d - T_E^{act}$ vs T_E^d curves for different noise levels in the system. The vertical dashed lines represent the uncontrolled MST for each noise level.

VI. CONCLUSIONS

In this work, a control strategy that could be used to control the mean switching time (MST) in a multistable dynamical system affected by external noise was presented. The main idea was to use an external control signal to obtain a desired MST. It was shown that the control strategy could be used to enhance or abate the MST by changing the action of the noise required to affect a transition. A specific controller, inspired by the most probable noise profile leading to transition, was proposed to control the MST to a desired value. The controller was analyzed in a 1D system, and it was shown that the controller can achieve any MST in a bounded interval whose limits are governed by the amount of control actuation available. The strategy was evaluated in simulations using two dynamical systems, the double-gyre flow and the damped pendulum. The results show that the controller is indeed able to obtain desired MSTs for various noise levels in the system including non-Gaussian noise.

ACKNOWLEDGMENTS

This work was funded by the Office of Naval Research (ONR) (Grant No. N000141712690) and the National Science Foundation (NSF) (Award Nos. CMMI-1418956, CMMI-1462884, DMS-1418956, and IIS-1253917).

REFERENCES

- ¹I. B. Schwartz, E. Forgoston, S. Bianco, and L. B. Shaw, "Converging towards the optimal path to extinction," *J. R. Soc. Interface* **8**, 1699–1707 (2011).
- ²G. T. Nieddu, L. Billings, J. H. Kaufman, E. Forgoston, and S. Bianco, "Extinction pathways and outbreak vulnerability in a stochastic ebola model," *J. R. Soc. Interface* **14**, 20160847 (2017).
- ³G. Nieddu, L. Billings, and E. Forgoston, "Analysis and control of pre-extinction dynamics in stochastic populations," *Bull. Math. Biol.* **76**, 3122–3137 (2014).
- ⁴M. Assaf, E. Roberts, and Z. Luthey-Schulten, "Determining the stability of genetic switches: Explicitly accounting for mRNA noise," *Phys. Rev. Lett.* **106**, 248102 (2011).
- ⁵R. V. Kohn, M. G. Reznikoff, and E. Vanden-Eijnden, "Magnetic elements at finite temperature and large deviation theory," *J. Nonlinear Sci.* **15**, 223–253 (2005).
- ⁶C. R. Heckman, A. M. Hsieh, and I. B. Schwartz, "Going with the flow: Enhancing stochastic switching rates in multigyre systems," *J. Dyn. Syst. Meas. Control* **137**, 031006 (2014).
- ⁷C. R. Heckman, M. A. Hsieh, and I. B. Schwartz, "Controlling basin breakout for robots operating in uncertain flow environments," in *Experimental Robotics: The 14th International Symposium on Experimental Robotics*, edited by M. A. Hsieh, O. Khatib, and V. Kumar (Springer International Publishing, 2016), pp. 561–576.
- ⁸E. Roberts, S. Be'er, C. Bohrer, R. Sharma, and M. Assaf, "Dynamics of simple gene-network motifs subject to extrinsic fluctuations," *Phys. Rev. E* **92**, 062717 (2015).
- ⁹R. P. Feynman and A. R. Hibbs, *Quantum Mechanics and Path Integrals* (McGraw-Hill Inc., 1965).
- ¹⁰M. I. Freidlin and A. D. Wentzell, *Random Perturbations of Dynamical Systems* (Springer-Verlag, 1984).
- ¹¹M. I. Dykman, E. Mori, J. Ross, and P. M. Hunt, "Large fluctuations and optimal paths in chemical-kinetics," *J. Chem. Phys.* **100**, 5735–5750 (1994).
- ¹²V. N. Smelyanskiy, M. I. Dykman, and R. S. Maier, "Topological features of large fluctuations to the interior of a limit cycle," *Phys. Rev. E* **55**, 2369–2391 (1997).
- ¹³B. E. Vugmeister and H. Rabitz, "Cooperating with nonequilibrium fluctuations through their optimal control," *Phys. Rev. E* **55**, 2522–2524 (1997).
- ¹⁴H. A. Kramers, "Brownian motion in a field of force and the diffusion model of chemical reactions," *Physica* **7**, 284–304 (1940).
- ¹⁵E. Forgoston, L. Billings, P. Yecko, and I. B. Schwartz, "Set-based corral control in stochastic dynamical systems: Making almost invariant sets more invariant," *Chaos* **21**, 013116 (2011).
- ¹⁶D. Kularatne, E. Forgoston, and M. A. Hsieh, "Exploiting stochasticity for the control of transitions in gyre flows," in *Robotics: Science and Systems* (Pittsburgh, PA, 2018).
- ¹⁷G. Veronis, "Wind-driven ocean circulation—Part 2. Numerical solutions of the non-linear problem," in *Deep Sea Research and Oceanographic Abstracts* (Elsevier, 1966), Vol. 13, pp. 31–55.
- ¹⁸V. Berdichevsky and M. Gitterman, "Josephson junction with noise," *Phys. Rev. E* **56**, 6340–6354 (1997).
- ¹⁹M. I. Freidlin and A. D. Wentzell, "On small random perturbations of dynamical system," *Russ. Math. Surveys* **25**, 1–55 (1970).
- ²⁰H. B. Chan, M. I. Dykman, and C. Stambaugh, "Switching-path distribution in multidimensional systems," *Phys. Rev. E* **78**, 051109 (2008).
- ²¹N. G. Van Kampen, *Stochastic Processes in Physics and Chemistry* (Elsevier, 1992).
- ²²C. W. Gardiner, *Handbook of Stochastic Methods for Physics, Chemistry and the Natural Sciences* (Springer-Verlag, Berlin, 2009).
- ²³E. Forgoston and R. O. Moore, "A primer on noise-induced transitions in applied dynamical systems," *SIAM Rev.* **60**, 969 (2018).